CME SAM

Cardiac Imaging

AJR FOCUS ON:

Cardiac Imaging: Part 1, MR Pulse Sequences, Imaging Planes, and Basic Anatomy

Daniel T. Ginat[1]
Michael W. Fong[2]
David J. Tuttle[1]
Susan K. Hobbs[1]
Rajashree C. Vyas[1]

OBJECTIVE. MRI is a well-established modality for evaluating congenital and acquired cardiac diseases. This article reviews the latest pulse sequences used for cardiac MRI. In addition, the standard cardiac imaging planes and corresponding anatomy are described and illustrated.

CONCLUSION. Familiarity with the basic pulse sequences, imaging planes, and anatomy pertaining to cardiac MRI is essential to formulate optimal protocols and interpretations.

Cardiac MRI is indicated for evaluating a wide variety of congenital and acquired heart diseases, including cardiac masses, myocardial ischemia or infraction, cardiomyopathies, valvular disease, coronary artery disease, pericardial disease, and complex congenital anomalies [1–3]. The high soft-tissue contrast, availability of a large FOV, multiplanar acquisition capability, and lack of ionizing radiation are particularly appealing features of cardiac MRI. However, the main limitation of cardiac MRI compared with CT is the evaluation of coronary calcifications.

General contraindications for cardiac MRI include iron particles in the globe and intracranial aneurysm clips [3]. Although also traditionally contraindicated for MRI because of concerns of arrhythmia and excess device heating, most patients with modern pacemakers and other types of implanted cardiac devices can safely undergo cardiac MRI examination at 1.5 T provided that appropriate precautions have been implemented [4, 5]. Pregnancy is considered a relative contraindication for cardiac MRI, although there are no known risks to the fetus. Except certain early models, valvular prostheses do not preclude cardiac MRI but their presence can degrade image quality [3].

There are certain technical challenges unique to cardiac MRI. Most notably is the rapid and complex motion of the heart and pulsatility of the great vessels due to normal contractility. In addition, the effects of respiratory motion and systolic ventricular blood velocities up to 200 cm/s further complicate cardiac imaging [6]. Nevertheless, these issues are generally mitigated by implementation of ECG (cardiac) gating; navigator echo respiratory gating; breath-hold techniques; rapid, high-performance gradients; improved field homogeneity; and advanced pulse sequences.

ECG gating can be either prospective or retrospective. Prospective gating consists of initiating image acquisition with R wave triggering. The advantage to this approach is that only the necessary data are collected. However, excessive heart rate variability limits the application of this technique. In addition, prospective gating is prone to artifacts that cause increased initial signal intensity, but increased signal intensity can be corrected using additional pulses during the dead time interval [7]. Retrospective gating involves continuous image acquisition throughout the cardiac cycle and selecting the desired data subsequently during post-processing. Although retrospective gating is less sensitive to heart rate fluctuations, retrospective gating is more time-consuming than prospective gating [7]. Navigator echo respiratory gating enables image acquisition during free breathing. An excitation pulse at the level of the diaphragm or heart is used to track patient breathing: Images are acquired only during end-expiration [7].

Numerous pulse sequences have been applied to cardiac MRI. To select the optimal protocol and to interpret cardiac MRI studies, the radiologist should understand the basic pulse sequences. In addition, the radiologist interpreting cardiac MRI studies should be familiar with basic cardiac anatomy and standard imaging planes. These topics are reviewed and illustrated in the following sections.

Keywords: anatomy, cardiac MRI, imaging planes, pulse sequences

DOI:10.2214/AJR.10.7231

Received January 31, 2010; accepted after revision May 30, 2010.

[1]Department of Imaging Science, University of Rochester Medical Center, 601 Elmwood Ave, Rm 3-4330, Rochester, NY 14642. Address correspondence to D. T. Ginat (ginatd01@gmail.com).

[2]Division of Cardiovascular Medicine, University of Southern California, Los Angeles, CA.

CME/SAM
This article is available for CME/SAM credit.
See www.arrs.org for more information.

AJR 2011; 197:808–815

0361–803X/11/1974–808

Pulse Sequences

Pulse sequences are software programs that encode the magnitude and timing of the radiofrequency pulses emitted by the MR scanner, switching of the magnetic field gradient, and data acquisition. The components of a pulse sequence are termed "imaging engines" and "modifiers" [8]. Imaging engines are integral features of a pulse sequence, whereas modifiers are optional additions. Imaging engines include fast spin-echo (FSE), gradient-echo (GRE), steady-state free precession (SSFP), echo-planar imaging (EPI), and single-shot versus segmented modes. Modifiers include fat suppression, inversion prepulse, saturation prepulse, velocity-encoded, and parallel imaging [8].

Dark Blood Imaging

Dark blood imaging refers to the low-signal-intensity appearance of fast-flowing blood and is mainly used to delineate anatomic structures. Traditionally, spin-echo (SE) sequences have been used for dark blood imaging. SE has been supplanted by the newer FSE and turbo spin-echo (TSE) techniques in cardiac imaging. Although these techniques have lower signal-to-noise ratio than SE, they enable rapid imaging, which minimizes the effects of respiratory and cardiac motion. Basic FSE and TSE sequences consist of radiofrequency pulses with flip angles (α) of 90° and 180° followed by acquisition of 1 or 2 signals (Fig. 1). FSE and TSE sequences can be T1- or T2-weighted acquired over a series of single or double R-R intervals. A potential source of artifact is slow-flowing blood, which can appear bright and can blend in with anatomic structures. Similarly, the presence of gadolinium can interfere with nulling of blood signal and should be administered after dark blood imaging. However, real-time nongated black blood sequences with gadolinium contrast administration have proven to be effective for evaluating myocardial ischemia [9].

Bright Blood Imaging

Bright blood imaging describes the high signal intensity of fast-flowing blood and is typically used to evaluate cardiac function. The main pulse sequences used for bright blood imaging include GRE and the more recently introduced, but related, technique termed "steady-state free precession" or "SSFP." GRE sequences (i.e., spoiled gradient recall [SPGR], turbo FLASH, turbo field echo, and fast-field echo [FFE]) are produced by emitting an excitation radiofrequency pulse that is usually less than 90°, followed by gradient reversals in at least two directions, which create an echo signal that can be detected (Fig. 2). SSFP sequences (i.e., fast imaging employing steady-state acquisition [FIESTA], fast imaging with steady-state precession [FISP], balanced FFE) are similar but incorporate a short TR with gradient refocusing that is less vulnerable to T2* effects compared with standard GRE. SSFP sequences can be executed rapidly while providing greater contrast-to-noise and signal-to-noise ratios than GRE sequences. EPI is another rapid sequence that involves the application of a single radiofrequency excitation pulse, usually with flip angles of less than 90° (Fig. 3). This sequence can also be combined with GRE. EPI is often used for functional assessment in cases in which arrhythmia precludes adequate gating.

Modifiers

Inversion recovery (IR) consists of applying additional 180° pulses. Double or triple IR can be used to further null signal from blood for black blood imaging, thereby improving contrast between the cardiac tissues and blood pool. This sequence is particularly useful for tumor imaging, delayed enhancement imaging, and coronary angiography. Fat suppression is accomplished in a similar manner, in which the inversion time of the additional selective 180° pulse is set to match the null time of fat.

Similar to IR, saturation-recover preparatory pulses also improve T1-weighted imaging. However, the saturation-recover pulse consists of applying a 90° flip angle and is less subject to signal intensity variations than IR techniques. Smaller flip angles can be used to maintain spatial resolution [9]. The saturation-recover pulse is often used in combination with GRE and hybrid GRE-EPI pulse sequences for perfusion-weighted imaging and myocardial tagging. Tagging involves labeling the myocardium with a low-signal-intensity grid. This enables quantification of myocardial strain and assessment of pericardial constriction. Tagging is also a more accurate method of assessing infarct-related dysfunction than wall thickness analysis [9]. Unfortunately, the grid tends to fade by early diastole.

Phase-contrast imaging with velocity-encoded imaging is a noncontrast technique that is frequently used to estimate pulmonary blood flow (Qp) and systemic blood flow (Qs) to calculate the pulmonary-to-systemic flow ratio (Qp:Qs) to determine shunt fraction. A Qp:Qs > 1.5 usually indicates a significant left-to-right shunt that requires surgical or percu-

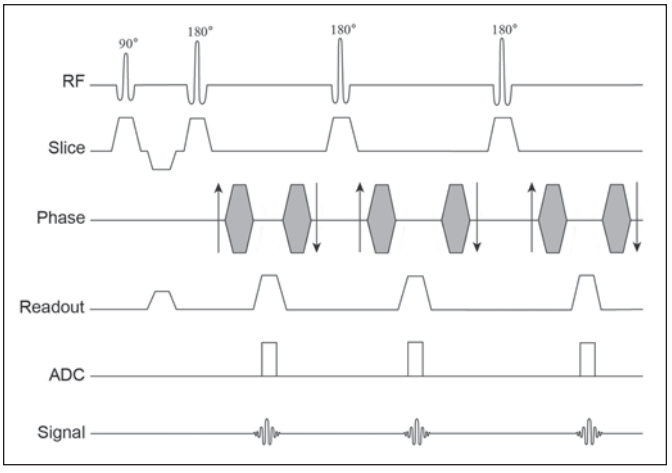

Fig. 1—Diagram shows fast spin-echo pulse sequence. RF = radiofrequency pulse, ADC = analog-to-digital converter.

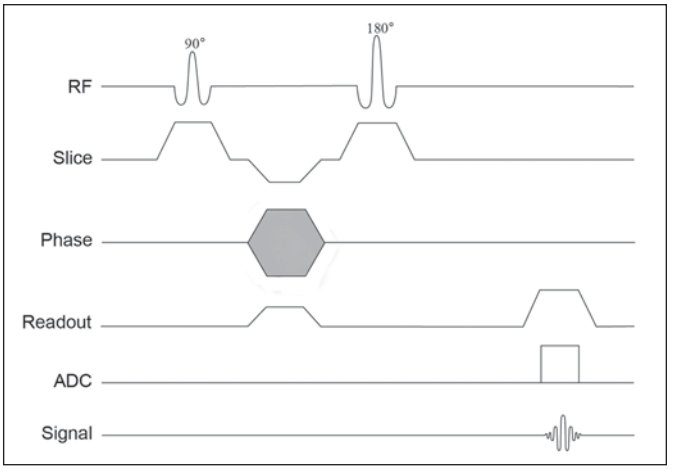

Fig. 2—Diagram shows steady-state free precession pulse sequence. RF = radiofrequency pulse, ADC = analog-to-digital converter.

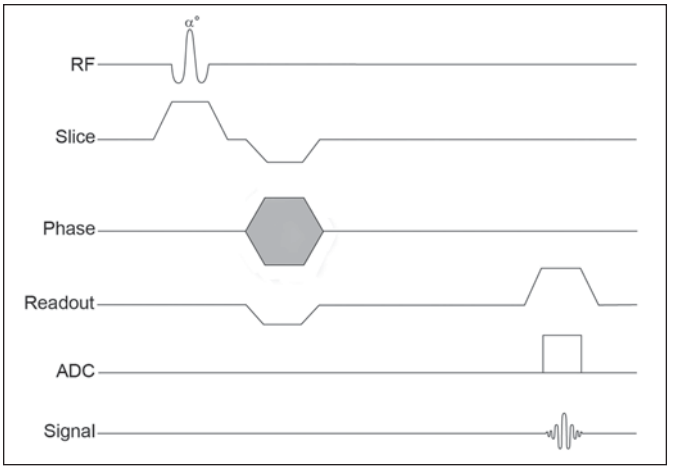

Fig. 3—Diagram shows echo-planar imaging pulse sequence. RF = radiofrequency pulse, ADC = analog-to-digital converter.

taneous correction. Velocity-encoded imaging can also be used to calculate regurgitant fractions and valve area using the continuity equation. The continuity equation uses the left ventricular outflow tract area and the velocity time integral of the aortic outflow tract and aortic valve. This technique is usually implemented via GRE pulse sequences (Fig. 4) and offers a temporal resolution on the order of 50 milliseconds [8]. The gradient strength must be selected to match the expected velocities. A velocity setting that is too low can cause aliasing, whereas a setting that is too high results in noisy, inaccurate measurements. Phase-contrast velocity-encoded imaging is susceptible to gradient field artifacts, and correction with phantoms is recommended to improve the accuracy of these measurements.

Parallel imaging techniques such as sensitivity-encoding (SENSE) and simultaneous acquisition of spatial harmonics (SMASH) enable accelerated imaging acquisition with short breath-hold times [3, 10]. Parallel imaging can be applied to most forms of cardiac imaging. These techniques make use of multiple coil arrays and sample limited portions of k-space over time. As a result, parallel imaging compromises the signal-to-noise ratio and is especially subject to artifacts [11].

Contrast-Enhanced Techniques and Other Applications of Pulse Sequences

The use of contrast material is an integral part of a myocardial viability study. Evaluation of myocardial viability with MRI is based on the phenomenon of delayed enhancement. This procedure consists of performing IR-GRE approximately 10 minutes after injection of a gadolinium-based contrast medium. Areas of myocardial infarct characteristically display enhancement when imaging is performed at an inversion time at which signal in the myocardium is maximally nulled (Fig. 5). Dynamic perfusion imaging is also useful for characterizing myocardial viability and is often carried out via EPI, which is a rapid sequence that is sometimes combined with GRE. For tumor imaging, T1-weighted IR-FSE pulse sequences are typically performed immediately after gadolinium injection.

Contrast-enhanced MRI can also be used for evaluating the coronary arteries and great vessels (Fig. 6). Maximum intensity projections (MIPs) and 3D vessel surface renderings are particularly useful adjuncts. Alternatively, ECG-gated balanced SSFP without arterial spin labeling can be applied as an unenhanced angiographic technique for imaging the aorta as well as the coronary arteries [12]. Arterial spin labeling can be further implemented to eliminate signal from venous flow. A limitation of SSFP for angiography is sensitivity to field inhomogeneities.

A basic MRI examination for evaluating suspected cardiac masses consists of static T2-weighted, T1-weighted, and gadolinium-enhanced T1-weighted sequences for anatomic characterization and a dynamic cine SSFP sequence for functional evaluation [13, 14]. In particular, the following five sequences should be included: cine SSFP, double IR T1-weighted FSE, double IR T2-weighted FSE, spectral presaturation with IR (SPIR), and gadolinium-enhanced T1-weighted GRE sequences [12]. In particular, intracavitary masses should be assessed with long–inversion time imaging (i.e., 500–600 ms) with gating every 3 or 4 R-to-R intervals to distinguish between tumor and thrombus. The signal from thrombus is generally maximally nulled much later than the signals from other tissues and can be readily distinguished using this technique. This combination of sequences often enables specific tumor characterization and may be helpful for distinguishing between malignant and benign tumors [14].

Imaging Planes and Anatomy

The two main coordinate systems used for cardiac MRI include the body (scanner) planes and the cardiac planes.

Body Planes

Body planes are oriented orthogonal to the long axis of the body and consist of axial, sagittal, and coronal planes (Fig. 7). These planes are used to derive the scout images and provide a qualitative overview of cardi-

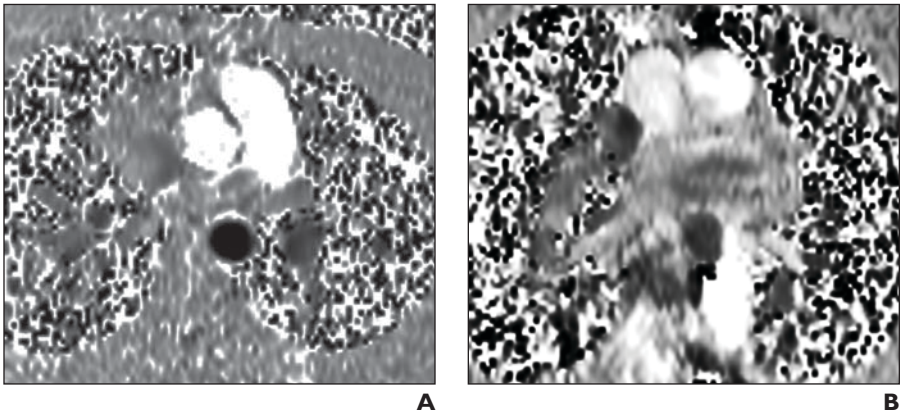

A B

Fig. 4—Phase-contrast images of a normal subject. **A** and **B,** Transverse aortic (**A**) and pulmonary artery (**B**) phase-contrast images.

ac morphology. The axial plane can depict the four chambers of the heart and the pericardium simultaneously. The sagittal plane can show the great vessels arising in continuity from the ventricles. The coronal plane can be used to assess the left ventricular outflow tract, the left atrium, and the pulmonary veins. However, the obliquity (≈ 45°) of these planes to the walls of the heart precludes accurate anatomic and functional characterization. Rather, such information should be obtained from the specialized cardiac planes.

Fig. 5—Two-chamber delayed enhancement view in a patient with a transmural infarct shows anterior wall, apex, and inferoapex in distribution of left anterior descending artery.

Cardiac Planes

The standard cardiac planes are established using the scout images and include short axis, horizontal long axis (four-chamber view), and vertical long axis (two-chamber view) (Fig. 8). These planes are prescribed along a line extending from the cardiac apex to the center of the mitral valve (long axis of the heart) using the axial body plane images. The short-axis plane extends perpendicular to this true long axis of the heart at the level of the mid left ventricle. The horizontal long axis is generated by selecting the horizontal plane that is perpendicular to the short axis, whereas the vertical long axis is prescribed along a vertical plane orthogonal to the short-axis plane. Ventricular volumetric measurements are routinely derived from the short-axis views [15].

Other commonly used planes include the oblique sagittal plane (parallel to the axis of the aorta), "three-points" plane (connects three points along a selected coronary artery), left ventricular outflow view (three-chamber view), and right ventricular outflow track view. The optimal planes used for evaluating the major structures and chambers of the heart are listed in Table 1.

Anatomy

The major cardiac structures that can be identified on MRI are listed in Table 2 and are illustrated on different imaging planes in Figure 9.

Right atrium—The morphologic right atrium is derived from the right atrial appendage and sinus venosus [16]. The sinus venosus has a smooth wall and receives the inferior vena cava and superior vena cava–coronary sinus, and

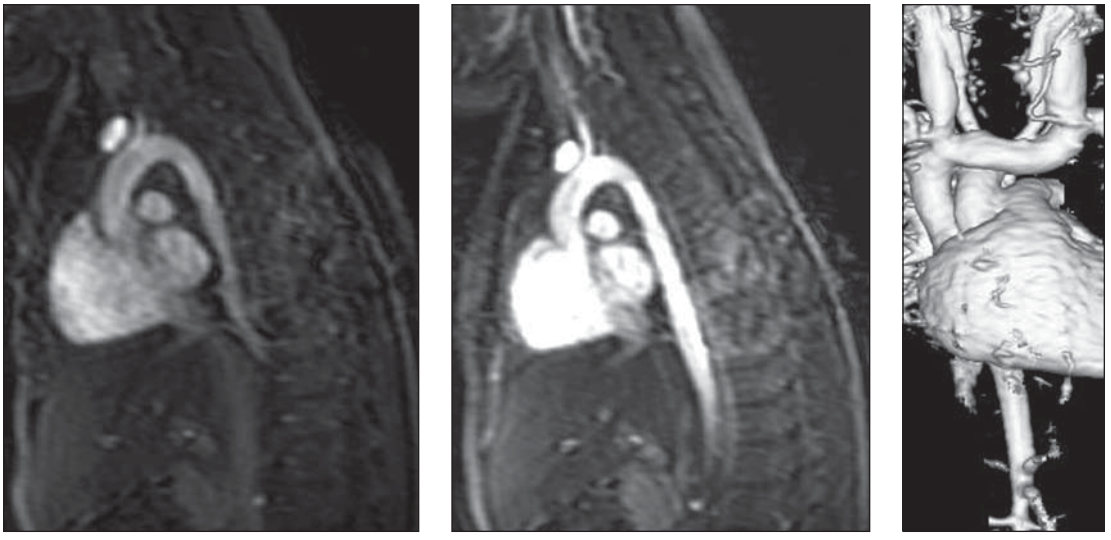

Fig. 6—Contrast-enhanced cardiac MRI.
A–C, Contrast-enhanced oblique sagittal view (**A**) and corresponding maximum intensity projection (**B**) and 3D surface-rendering (**C**) images of aorta show double aortic arch. Maximum-intensity projections (MIPS) and 3D vessel surface renderings are particularly useful adjuncts.

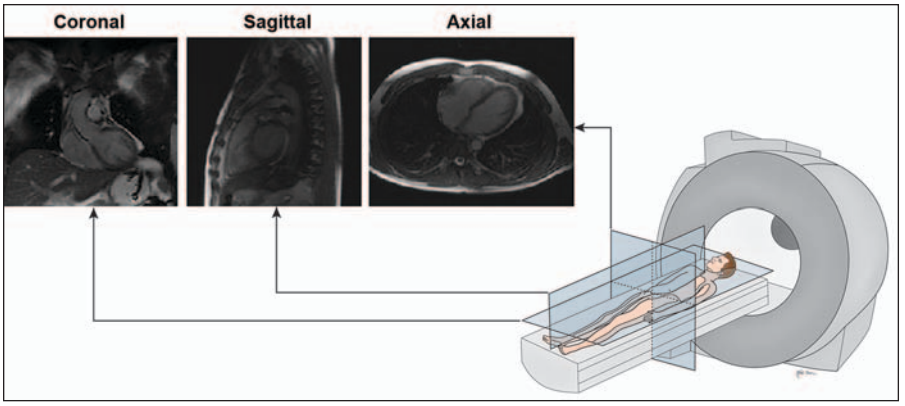

Fig. 7—Schematic shows orientation of major body planes with respect to patient and their corresponding appearance on bright blood imaging sequences.

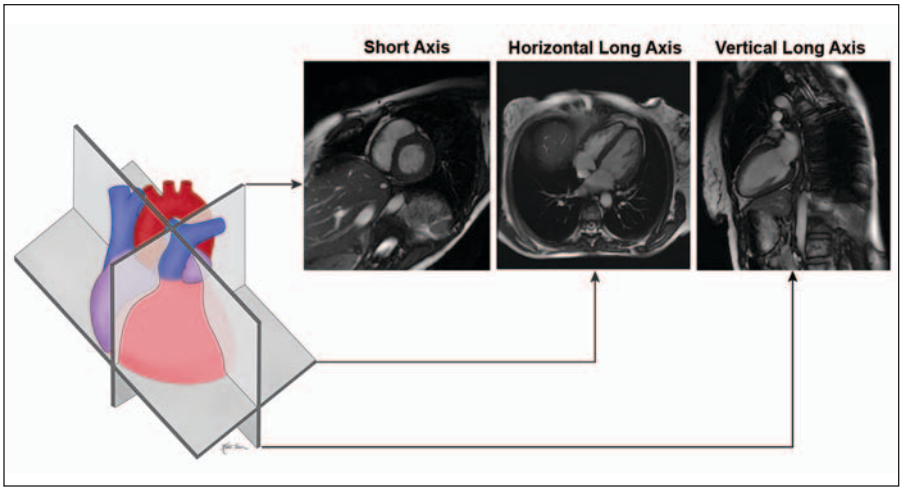

Fig. 8—Schematic shows orientation of major cardiac planes with respect to heart and their corresponding appearance on bright blood sequences.

the right atrial appendage is triangular-shaped with a wide opening and contains rough trabeculations or pectinate muscles. These two components of the right atrium are separated by the crista terminalis (terminal crest). The crista terminalis is readily visualized on both bright and dark blood sequences and appears isointense to the myocardium. A prominent crista terminalis can mimic a mass, as shown in Figure 10. However, the location and signal characteristics on MRI can help confirm that this structure is indeed normal cardiac tissue [17]. The valves of the coronary sinus (thebesian valve) and inferior vena cava (eustachian valve) are also readily apparent on MRI.

Right ventricle—The right ventricle receives blood from the right atrium and consists of inlet, outlet, and apical portions [16]. The inlet contains the tricuspid valves and associated chordal attachments. Attachment of the chords to the septum is characteristic of the tricuspid valve. The apical portion of the right ventricle is trabeculated, whereas the

TABLE 1: Optimal Planes for Imaging Cardiac Structures and Chambers

Structure or Chamber	Imaging Planes
Left ventricle	Four-chamber view, horizontal long- and short-axis views, and LVOT view
Right ventricle	Right-sided horizontal long-axis view, short-axis view, and RVOT view
Left atrium	Horizontal long-axis view, LVOT view, and four-chamber view
Right atrium	Axial, coronal, and right -sided horizontal long-axis planes
Aorta	Oblique sagittal plane
Main pulmonary artery	Sagittal plane of the RVOT view
Coronary arteries	Three-point planes

Note—LVOT = left ventricular outflow tract, RVOT = right ventricular outflow tract.

TABLE 2: Summary of Normal Cardiac Anatomy

Structure	Components
Right atrium	Right atrial appendage, pectinate muscles, crista terminalis
Left atrium	Left atrial appendage, pectinate muscles
Right ventricle	
Inlet	Tricuspid valve
Outlet	Pulmonary valve
Apical region	Papillary muscles and moderator band
Left ventricle	
Inlet	Mitral valve
Outlet	Aortic valve
Apical region	Papillary muscles
Coronary arteries	
RCA	PDA, conal branch, sinus node artery, right marginal branch, and posterolateral branch
Left main coronary artery	LCA and left circumflex artery
LCA	Diagonal and septal branches
Left circumflex artery	Obtuse marginal branches; sometimes sinus node artery and PDA in a left dominant or codominant system

Note—RCA = right coronary artery, PDA = posterior descending artery, LCA = left coronary artery.

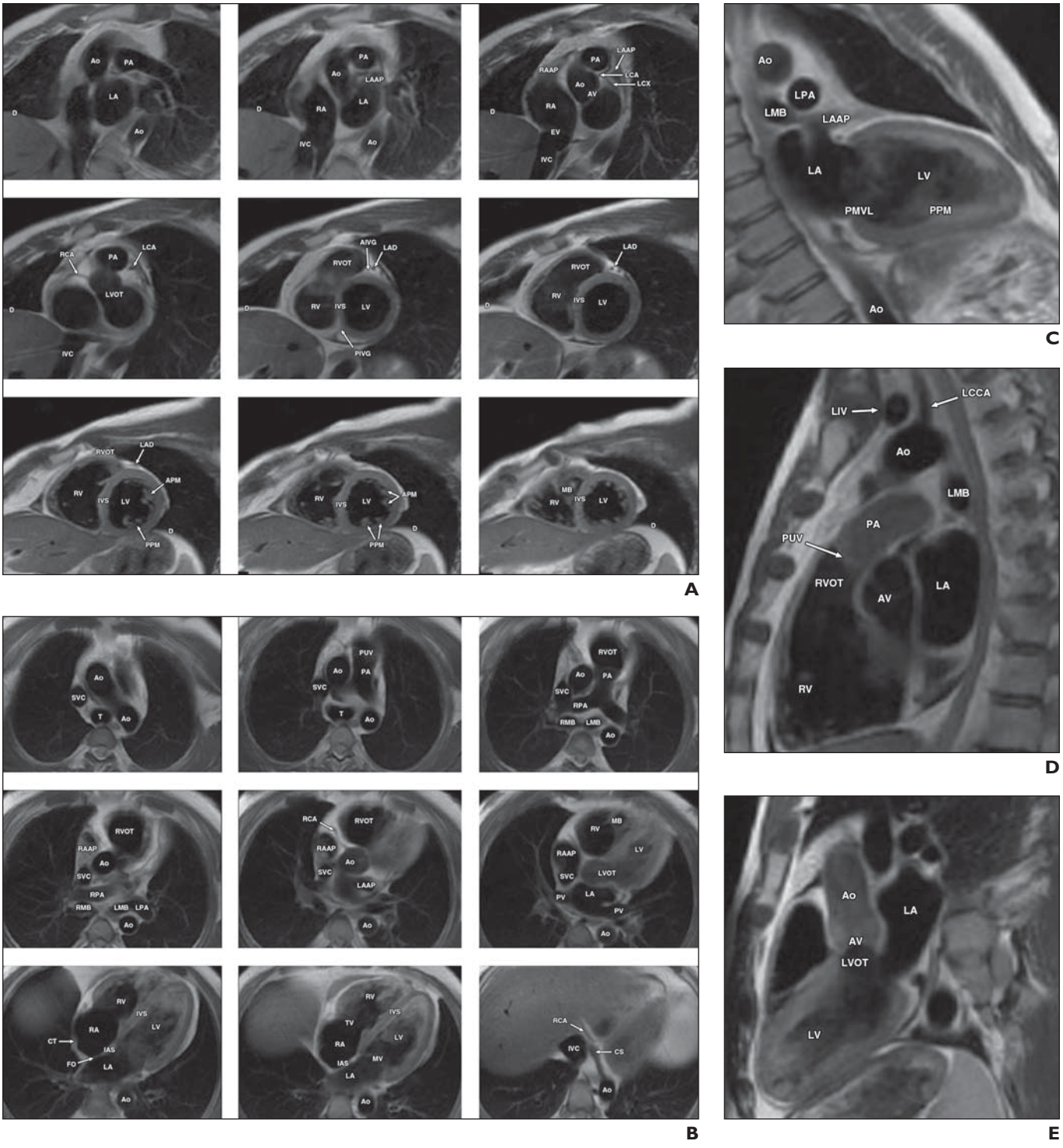

Fig. 9—Normal cardiac MRI anatomy shown in healthy subject. Ao = aorta, AIVG = anterior interventricular groove, APM = anterior papillary muscle, AV = aortic valve, CS = coronary sinus, CT = crista terminalis, D = diaphragm, EV = eustachian valve, FO = fossa ovalis, IAS = interatrial septum, IVC = inferior vena cava, IVS = interventricular septum, LA = left atrium, LAAP = left atrial appendage, LAD = left anterior descending artery, LCA = left coronary artery, LCCA = left common carotid artery, LCX = left circumflex artery, LIV = left innominate vein, LMB = left mainstem bronchus, LPA = left pulmonary artery, LV = left ventricle, LVOT = left ventricular outflow tract, MB = moderator band, MV = mitral valve, PA = pulmonary artery, PMVL = posterior mitral valve leaflet, PPM = posterior papillary muscle, PUV = pulmonary valve, RA = right atrium, RAAP = right atrial appendage, RCA = right coronary artery, RMB = right mainstem bronchus, RPA = right pulmonary artery, RV = right ventricle, RVOT = right ventricular outflow tract, SVC = superior vena cava, T = trachea, TV = tricuspid valve, PV = pulmonary vein.
A–E, Short-axis (**A**), horizontal long-axis (**B**), two-chamber (**C**), right ventricular outflow tract (**D**), and left ventricular outflow tract (**E**) views.

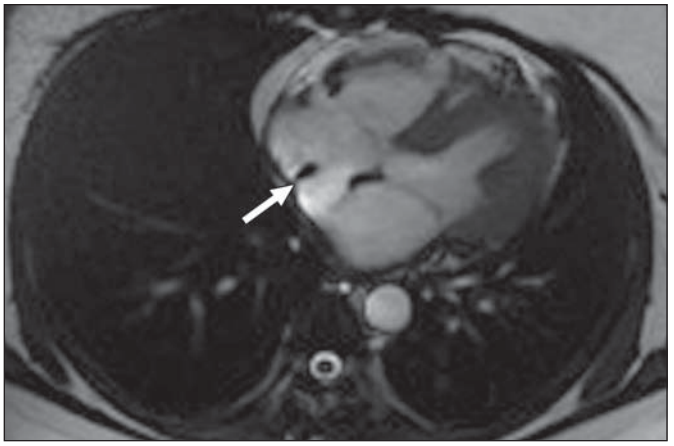

Fig. 10—Normal cardiac MRI anatomy shown in healthy subject. Axial fast imaging employing steady-state acquisition image shows prominent crista terminalis (*arrow*). This finding is normal variant not to be confused with tumor or thrombus.

outlet is smooth and leads to the pulmonary artery. The right ventricle also contains the moderator band, which courses from the apical portion at the anterior papillary muscle insertion to the interventricular septum.

Left atrium—The left atrium is the most posterior and superior chamber and receives pulmonary venous return [16]. The left atrium is also attached to the left atrial appendage, which is more elongated and narrower than the right atrial appendage. The left atrium is smaller and contains fewer trabeculations than the right atrium. The interatrial septum separates the right and left atria and features the fossa ovalis, which appears as an area of focal thinning.

Left ventricle—The left ventricle comprises inlet, apical, and outlet segments and is separated from the right ventricle by the interventricular septum [16]. The septum normally bulges toward the right ventricle. Consequently, on short-axis views, the left ventricle has a rounded profile. The left ventricle inlet and outlet are continuous with one another and include the mitral and aortic valves, respectively. The apical region of the left ventricle contains the two papillary muscles, which are larger than those in the right ventricle. In adults, the lateral wall of the normal left ventricle should measure less than 1 cm in thickness [3].

Coronary arteries—The coronary arteries arise from the aortic sinuses, just distal to the aortic valve. The right coronary artery (RCA) courses along the atrioventricular groove and is dominant in approximately 85% of individuals, giving rise to the posterior descending artery (PDA), which courses along the posterior interventricular sulcus toward the apex. The RCA also supplies the conal branch, right marginal branches, posterolateral ventricular branch, and frequently the sinus node artery.

The left main coronary artery is a short trunk that supplies the left anterior descending (LAD) and left circumflex arteries. In up to 30% of individuals an additional ramus intermedius artery arises from the bifurcation of the left main coronary artery [16]. The LAD courses along the anterior interventricular sulcus and give rise to the diagonal and septal branches. The left circumflex artery supplies the obtuse marginal branches and sometimes supplies the sinus node artery and PDA in a left-dominant or codominant system.

References

1. Hendel RC, Patel MR, Kramer CM, et al.; American College of Cardiology Foundation Quality Strategic Directions Committee Appropriateness Criteria Working Group. American College of Radiology; Society of Cardiovascular Computed Tomography; Society for Cardiovascular Magnetic Resonance; American Society of Nuclear Cardiology; North American Society for Cardiac Imaging; Society for Cardiovascular Angiography and Interventions; Society of Interventional Radiology. ACCF/ACR/SCCT/SCMR/ASNC/NASCI/SCAI/SIR 2006 appropriateness criteria for cardiac computed tomography and cardiac magnetic resonance imaging: a report of the American College of Cardiology Foundation Quality Strategic Directions Committee Appropriateness Criteria Working Group, American College of Radiology, Society of Cardiovascular Computed Tomography, Society for Cardiovascular Magnetic Resonance, American Society of Nuclear Cardiology, North American Society for Cardiac Imaging, Society for Cardiovascular Angiography and Interventions, and Society of Interventional Radiology. *J Am Coll Cardiol* 2006; 48:1475–1497
2. Pennell DJ, Sechtem UP, Higgins CB, et al. European Society of Cardiology; Society for Cardiovascular Magnetic Resonance. Clinical indications for cardiovascular magnetic resonance (CMR): Consensus Panel report. *J Cardiovasc Magn Reson* 2004; 6:727–765
3. Boxt LM. Cardiac MR imaging: a guide for the beginner. *RadioGraphics* 1999; 19:1009–1025; discussion, 1026–1028
4. Martin ET, Coman JA, Shellock FG, Pulling CC, Fair R, Jenkins K. Magnetic resonance imaging and cardiac pacemaker safety at 1.5-Tesla. *J Am Coll Cardiol* 2004 7; 43:1315–1324
5. Nazarian S, Roguin A, Zviman MM, et al. Clinical utility and safety of a protocol for noncardiac and cardiac magnetic resonance imaging of patients with permanent pacemakers and implantable-cardioverter defibrillators at 1.5 Tesla. *Circulation* 2006; 114:1277–1284
6. Reeder SB, Du YP, Lima JA, Bluemke DA. Advanced cardiac MR imaging of ischemic heart disease. *RadioGraphics* 2001; 21:1047–1074
7. Scott AD, Keegan J, Firmin DN. Motion in cardiovascular MR imaging. *Radiology* 2009; 250:331–351
8. Kim HW, Klem I, Kim RJ. Detection of myocardial ischemia by stress perfusion cardiovascular magnetic resonance. *Cardiol Clin* 2007; 25:57–70, vi
9. Detsky JS, Graham JJ, Vijayaraghavan R, et al. Free-breathing, nongated real-time delayed enhancement MRI of myocardial infarcts: a comparison with conventional delayed enhancement. *J Magn Reson Imaging* 2008; 28:621–625
10. Vitanis V, Manka R, Boesiger P, Kozerke S. Accelerated cardiac perfusion imaging using k-t SENSE with SENSE training. *Magn Reson Med* 2009; 62:955–965
11. Saremi F, Grizzard JD, Kim RJ. Optimizing cardiac MR imaging: practical remedies for artifacts. *RadioGraphics* 2008; 28:1161–1187
12. Miyazaki M, Lee VS. Nonenhanced MR angiography. *Radiology* 2008; 248:20–43
13. Sparrow PJ, Kurian JB, Jones TR, Sivananthan MU. MR imaging of cardiac tumors. *RadioGraphics* 2005; 25:1255–1276
14. Syed IS, Feng D, Harris SR, et al. MR imaging of cardiac masses. *Magn Reson Imaging Clin N Am* 2008; 16:137–164, vii
15. Forbat SM, Sakrana MA, Darasz KH, El-Demerdash F, Underwood SR. Rapid assessment of left ventricular volume by short axis cine MRI. *Br J Radiol* 1996; 69:221–225
16. Bogaert J, Dymarkowski S, Taylor AM, eds. *Clinical cardiac MRI*. New York, NY: Springer-Verlag, 2005
17. Mirowitz SA, Gutierrez FR. Fibromuscular elements of the right atrium: pseudomass at MR imaging. *Radiology* 1992; 182:231–233

FOR YOUR INFORMATION

The reader's attention is directed to part 2 accompanying this article, titled "Cardiac Imaging: Part 2, Normal, Variant, and Anomalous Configurations of the Coronary Vascular," which begins on page 816.

FOR YOUR INFORMATION

The Self-Assessment Module accompanying this article can be accessed via www.ajronline.org at the article link labelled "CME/SAM."

The American Roentgen Ray Society is pleased to present these Self-Assessment Modules (SAMs) as part of its commitment to lifelong learning for radiologists. Each SAM is composed of two journal articles along with questions, solutions, and references, which can be found online. Read each article, then answer the accompanying questions and review the solutions online. After submitting your responses, you'll receive immediate feedback and benchmarking data to enable you to assess your results against your peers.

Continuing medical education (CME) and SAM credits are available in each issue of the *AJR* and are ***free to ARRS members. Not a member?*** Call 1-866-940-2777 (from the U.S. or Canada) or 703-729-3353 to speak to an ARRS membership specialist and begin enjoying the benefits of ARRS membership today!